Quantum-critical scaling properties of the two-dimensional random-singlet state

Lu Liu [1], Wenan Guo [2,3,*] and Anders W. Sandvik [4,1,†]

[1]*Beijing National Laboratory for Condensed Matter Physics, Institute of Physics, Chinese Academy of Sciences, Beijing 100190, China*
[2]*Department of Physics, Beijing Normal University, Beijing 100875, China*
[3]*Beijing Computational Science Research Center, Beijing 100193, China*
[4]*Department of Physics, Boston University, 590 Commonwealth Avenue, Boston, Massachusetts 02215, USA*

Using quantum Monte Carlo simulations, we study effects of disorder on the $S = 1/2$ Heisenberg model with exchange constant J on the square lattice supplemented by multispin interactions Q. It was found recently [L. Liu *et al.*, Phys. Rev. X **8**, 041040 (2018)] that the ground state of this J-Q model with random couplings undergoes a quantum phase transition from the Néel antiferromagnetic state into a randomness-induced spin-liquid-like state that is a close analog to the well known random-singlet (RS) state of the Heisenberg chain with random couplings. This 2D RS state arises from a spontaneously symmetry-broken fourfold degenerate columnar valence-bond solid that is broken up by the disorder into finite domains, with spinons localized at topological defects. The interacting spinons form a critical collective many-body state without magnetic long range order but with the mean spin-spin correlations decaying with distance r as r^{-2}, as in the one-dimensional RS state. The dynamic exponent $z \geqslant 2$, varying continuously with the model parameters. In this work, we further investigate the properties of the RS state in the J-Q model with random Q couplings. We study the temperature dependence of the specific heat and various susceptibilities for large enough systems to reach the thermodynamic limit. We also analyze the size dependence of the critical magnetic order parameter and its susceptibility in the ground state. For all these quantities, we find consistency with the conventional quantum-critical scaling laws when the condition implied by the r^{-2} form of the spin correlations is imposed. In particular, all the different quantities can be explained by the same value of the dynamic exponent z at fixed model parameters. We argue that the RS state identified in the J-Q model corresponds to a generic renormalization group fixed point that can be reached in many quantum magnets with random couplings and that it has already been observed experimentally.

I. INTRODUCTION

Effects of disorder and impurities play an important role in quantum many-body physics, not only because of their perturbing effects on uniform systems but also because the interplay of disorder and quantum fluctuations can lead to completely different states. Prominent examples are Anderson localization of electrons [1] and its proposed generalization to many-body localization in interacting systems [2–6]. Another interesting and well known state induced by disorder is the random singlet (RS) state in one-dimensional (1D) spin chains. The RS state is the fixed point of the simple but powerful strong-disorder renormalization group (SDRG) method [7–10], where pairs of strongly coupled spins are successively decimated. The fixed point is an infinite-randomness fixed point (IRFP), where the effective strength of the randomness (the width of the coupling distribution on a logarithmic scale) increases to infinity without bounds under the renormalization group (RG) flow.

The 1D RS state resulting from the SDRG method for a system such as the $S = 1/2$ antiferromagnetic Heisenberg chain with random couplings is a special 'frozen' config-

uration of random singlet spin pairs (valence bonds), and this state accurately represents the true ground state, which is a superposition of valence-bond coverings. The distance between two spins in a singlet is typically short, but there are rare instances of very long valence bonds that cause the mean spin correlations to decay with distance as r^{-2}, while the typical correlations decay exponentially. A striking property of the IRFPs is that the dynamic exponent z is infinite, leading to unconventional dynamical scaling properties. In this paper we will present a detailed numerical characterization of a two-dimensional (2D) state of $S = 1/2$ spins that is in many respects similar to the 1D RS state, though it has finite, but large, dynamic exponent.

A. Ground states of 2D random quantum magnets

The 1D RS phase is broadly realized in random spin chains with different symmetries, not only with the fully rotationally invariant Heisenberg (XXX) interactions but also in anisotropic XXZ chains and in the transverse-field Ising model (TFIM) [9]. In gapless host systems such as the $S = 1/2$ XXX and XX chains, even infinitesimal randomness drives the system asymptotically into the RS phase, while in uniform gapped systems (e.g., the integer-S Heisenberg chains with Haldane gaps) a critical disorder (width of the coupling distribution) is required [11]. In spontaneously dimerized
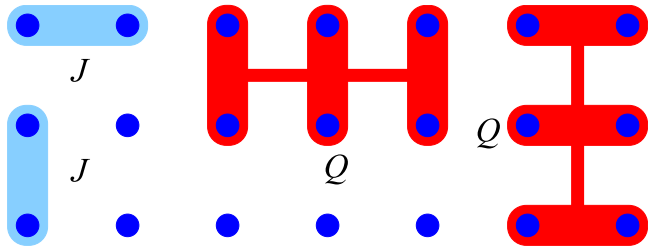
*waguo@bnu.edu.cn
†sandvik@bu.edu

FIG. 1. Illustration of the terms in the 2D J-Q model studied in this paper. Sites on the square lattice are shown as blue dots. The light blue bars represent the J terms while the groups of three connected red bars represent the products of three singlet projectors constituting each Q term.

systems with random couplings, such as the frustrated J_1-J_2 Heisenberg chain [12] or the J-Q chain [13] (a 1D variant of the model studied in this paper, which is illustrated in Fig. 1), domain walls with localized spinons form for any disorder strength and those spinons can form the IRFP-RS state in some cases [13] (and other states formed by the spinons have also been proposed [12]).

In two-dimensional (2D) systems, although IRFPs have been identified in TFIMs [14], no convincing evidence of such a state has been reported in 2D quantum magnets with SU(2) invariant interactions [15–19]; only a spurious IRFP was pointed out in Ref. [20]. Unlike the 1D case, an RS state is not obtained in the 2D Heisenberg model with bond randomness if all couplings remain antiferromagnetic (i.e., in the absence of frustration), with the Néel ground state surviving any strength of such disorder [21]. The robustness of the 2D Néel state is also exemplified by the site diluted system, which remains ordered all the way to the percolation point [22]. Interesting quantum states can be observed at the percolation points in site and bond diluted systems [23–27], and in some systems with two spins per unit cell in the clean limit, gapless disordered Griffiths phases have been observed [28]. SDRG studies of various Heisenberg systems have found what appear to be finite-randomness fixed points [15–19]. We note that the SDRG method can be applied generally, but if the decimation process does not flow to an IRFP, it is not clear whether the resulting state has any bearing on the true ground state. In particular, it is not known whether a finite-disorder fixed point [29] is correctly reproduced by the method.

Some frustrated quantum spin systems with random couplings have been shown to host spin-glass states, where, in analogy with classical spin models, there is no spatial order but the individual spin expectation values $\langle \mathbf{S}_i \rangle$ are frozen in time [30]. However, while some 2D $S = 1/2$ TFIMs with short-range interactions definitely exhibit spin glass behavior [31,32], no convincing case of SU(2) short-range interactions producing spin glasses have been presented. Analytical calculations with long-range interactions or some extension of the symmetry group, e.g., SU(N), have demonstrated spin glasses [30,33,34], but the relevance of such solutions to short-range interacting SU(2) spins is not clear. Nevertheless, it has been proposed that models such as the 2D Heisenberg with random nearest-neighbor couplings (with mixed signs of the couplings to introduce frustration) can host spin glass

phases, e.g., based on numerical exact diagonalization (ED) of small systems [35]. Extrapolating the properties based on ED to the thermodynamic limit is challenging, however, and other interpretations are also possible.

Alternatives to spin glass states have been proposed in the generic context of random frustrated interactions. In long-range interacting models a "spin fluid" phase with $\langle \mathbf{S}_i \rangle = 0$ and unusual dynamic properties similar to the marginal Fermi liquid was proposed [33], but again these properties do not necessarily carry over to short-range interacting $S = 1/2$ spins. Numerical studies of $S = 1/2$ systems with short-range interactions on various lattices have suggested states such as the valence-bond glass [36,37] and the randomness-induced quantum spin liquid [38–46]. The latter series of works includes also the square-lattice J_1-J_2 Heisenberg model [42], for which a spin glass ground state had previously been proposed [35]. Terms such as "valence-bond glass" and "randomness-induced spin liquid" do not yet have completely well defined meanings in terms of unique system properties related to specific RG fixed points in two space dimensions. It nevertheless appears that 2D states exist that have no spatial order, are not spin glasses (i.e., $\langle \mathbf{S}_i \rangle = 0$), but are gapless and in some ways similar to the 1D RS state. We will here characterize such a state in detail, based on a model amenable to quantum Monte Carlo (QMC) simulations (Fig. 1).

B. Routes to the 2D random-singlet state

Recently, two independent works using different techniques [47,48] pointed out that a state similar to the 1D RS state can be obtained by starting from a 2D valence-bond solid (VBS) state, i.e., a gapped state in which lattice symmetries are spontaneously broken due to the formation of a singlet pattern. Due to the Imry-Ma argument for disorder in systems with discrete symmetry breaking [49], extended to quantum systems, the VBS pattern is destroyed for any finite amount of coupling disorder, and in such a "broken VBS" topological defects along with unpaired spins (before interactions are considered) form localized spinons. These spinons, which are related to the spinons in clean VBS systems associated with deconfined quantum-critical points [50,51], are coupled to each other via effective interactions mediated by the host system, and the question is then what kind of magnetic subsystem they give rise to.

Kimchi *et al.* [47] argued that a state similar to the 1D RS state can form if the host system is frustrated, e.g., in the Heisenberg model on the triangular lattice, though eventually, at the lowest energy scales, a spin glass state may form (though no actual evidence was presented for a spin glass). They also suggested that an unfrustrated (bipartite) host system does not support the RS state but leads to antiferromagnetically ordered spinons. In our previous work with collaborators [48], we considered a "designer" J-Q model, illustrated in Fig. 1, and demonstrated that its VBS state in the presence of coupling disorder leads to domains and localized spinons, but there were no signs of the spinons forming long-range order. Instead, it was found that the spin correlations always decay with distance as r^{-2}, as in the 1D RS state, and quantum-critical scaling properties at finite temperature T were also identified. All scaling properties were explained

with a dynamic exponent which takes the value $z = 2$ at the transition from the Néel state and grows inside the RS phase. Values up to $z \approx 7$ were found in the *J-Q* model, and there is likely no upper bound in principle in an extended model space. We also presented arguments based on spinon pairing and domain-wall mediated interactions as to why no ordering takes place. The identified RS scaling properties then correspond to an asymptotic RG fixed point. We also suggested that this RS fixed point found in a system without traditional frustration (but with other forms of competition between different interactions) may be the same as the one identified by Kimchi *et al.* in frustrated models [47] and which was also argued to be realized in some materials [52] that had previously been regarded as quantum spin liquids [53] or quantum spin glasses [54].

The existence of a generic disorder-induced spin liquid had previously been argued based on numerical ED studies by Kawamura and collaborators [38–42]. The method only allows access to small system sizes, and it is difficult to interpret the results and extract long-distance and low-energy properties. ED results had previously been interpreted in terms of a spin glass [35]. The state studied in these ED works may actually be equivalent, in the RG sense, to the RS state discussed in Refs. [47,48]. It was also recently proposed that the starting point of the randomness-perturbed VBS state, where there is still substantial short-range VBS correlations and the spinons form a dilute subsystem, can be regarded as a weak-disorder variant of the state originating from strong randomness in frustrated systems [43]. There may potentially be no phase transition separating the weak and strong disorder cases, and instead one can think of continuously shrinking the VBS domains discussed in Refs. [47,48] until the domains become so small that it would be meaningless to consider them as domains. Instead the random valence-bond configurations may become more akin to a valence-bond glass [36,37]. The crucial point here is whether the localized spinons of the weak-disorder regime survive also at strong disorder. Indeed, also in the ED studies, "orphan spins" were identified that may be those spinons [38–43], though their role in forming the RS state was less clear because of the small system sizes and smaller distance between the orphan spins than between the spinons in the limit of large VBS domains [48]. Anderson localization of singlets had also been proposed as the mechanism responsible for the formation of RS state [40].

A very recent study based on a semiclassical approach gives support to the notion that spin glasses in classical frustrated systems transform into states akin to the 1D RS state when strong quantum effects are included [55] and that the mechanism of starting from the VBS states to understand such a 2D RS state [47,48] also is valid for systems that are not VBS ordered in the clean limit, e.g., the frustrated Heisenberg model on the triangular lattice (which has three-sublattice antiferromagnetic order for all spin values S).

If the RS state identified in the *J-Q* model indeed corresponds to the same fixed point as in the frustrated systems, for which further evidence based on density matrix renormalization group (DMRG) calculations has been presented recently [46], then this fixed point, as well as the phase transition into the Néel state, can be fully characterized in detail using QMC simulations. This is the *designer Hamiltonian* approach

[56] of studying specifically tailored lattice models that do not necessarily correspond to microscopic descriptions of specific materials but enables reliable calculations of universal properties.

C. Paper motivation and outline

The motivation for the present work is to test quantum-critical scaling laws in the random *J-Q* model to a higher degree than what was previously done in Ref. [48]. On the basis of such results we can make definite predictions for the RS phase that can be tested also in other models with different methods, as well as in materials. Because of the very significant computational efforts required, we focus on a single point inside the RS phase and study very large systems down to ultralow temperatures, in order to reliably obtain the asymptotic temperature dependence of the specific heat (which was not calculated in our previous work) and various susceptibilities (for which we report much improved results). For the same set of model parameters, we also study the ground state of systems on smaller lattice sizes (lengths) L and carry out finite-size scaling analysis. The $T > 0$, $L \to \infty$ scaling properties are fully consistent with the finite-L, $T \to 0$ finite-size behaviors with the same dynamic exponent $z \approx 4.0$, thus supporting a finite-disorder fixed point with formally conventional scaling behavior but with a large dynamic exponent z and spin correlations decaying universally as r^{-2} (for which we also show additional evidence here).

The paper is organized as follows: In Sec. II, we introduce the random-Q *J-Q* model. In Sec. III, we present scaling results for the specific heat, which we obtain by analyzing the internal energy density. In Sec. IV, we show results for the temperature dependent local, uniform, and staggered susceptibilities, extracting the asymptotic low-temperature forms in the thermodynamic limit. In Sec. V we discuss the staggered structure factor and susceptibility for smaller systems in the ground state, from which we extract an independent estimate of the dynamic exponent z. We conclude in Sec. VI with a discussion of the relevance of our findings to the present status of the 2D RS state, including possible experimental realizations.

II. 2D RANDOM *J-Q* MODEL AND SIMULATION METHOD

The *J-Q* model on a 2D square lattice has nearest-neighbor antiferromagnetic exchange J along with multispin interactions of strength Q [57] expressed using products of singlet projectors. We here study the variant in which the Q terms are products of three singlet projectors, also called the *J-Q_3* model [58], with the Hamiltonian defined as

$$H = -J \sum_{\langle ij \rangle} P_{ij} - Q \sum_{\langle ijklmn \rangle} P_{ij} P_{kl} P_{mn}, \tag{1}$$

where P_{ij} is the singlet projector for two $S = 1/2$ spins at sites i and j,

$$P_{ij} = \tfrac{1}{4} - \mathbf{S}_i \cdot \mathbf{S}_j. \tag{2}$$

In the Hamiltonian Eq. (1), $\langle ij \rangle$ indicates nearest-neighbor sites, and the index pairs ij, kl, and mn in $\langle ijklmn \rangle$ form three parallel bonds on horizontal or vertical stacks, as illustrated in

Fig. 1. The summations are over all nearest neighbors for the J terms and all translations of the vertical and horizontal stacks for the Q terms, so that the Hamiltonian does not break any lattice symmetries.

In the clean system, the J and Q terms compete with each other, individually having different ground states, leading to a phase transition from the standard Néel ordered ground state for small Q/J to the spontaneously dimerized columnar VBS state for large Q/J [51,57,58]. Such a Néel–VBS transition appears to realize the deconfined quantum criticality (DQC) scenario [59,60], a continuous order–order transition beyond the conventional Landau-Ginzburg-Wilson paradigm according to which the transition should be generically first order. While we will not discuss the quantum phase transition in the present work, the Néel–VBS transition may be considered the clean limit of the transition between the Néel state and the RS state forming due to disorder in either the J or Q terms [48].

To study effects of disorder, we here introduce randomness in the Q terms, choosing the strength of each of them to be either 0 or $2Q$ at random with equal probability for the two cases; then the mean strength $\bar{Q}$ of these interactions is still Q, which we take as our tuning parameter. We define the energy unit with $J = 1$. For this random-Q model, in our previous work we detected a quantum phase transition from the Néel phase to the RS phase upon increasing Q [48], with the critical point located at $Q_c \approx 1.2$. At the critical point, a dynamic exponent consistent with $z = 2$ was found. The entire RS phase is a critical state without magnetic long range order, with the mean spin-spin correlations decaying with distance r as r^{-2}. We confirmed this behavior for several points inside the RS phase, not only for the model with random bimodal Q but also with bimodal J and with continuous distributions of the couplings. We found consistently that $z \approx 2$ on the AFM–RS phase boundary (most likely $z = 2$ exactly), and z grows monotonically on moving deeper into the RS phase. Thus, while z can become large, this RS state does not correspond to an IFRP as the 1D variant [7–9]. In Sec. VI we will further discuss why the term RS state is still an appropriate way to characterize the state.

Our main aim here is to study several different quantities at high statistical precision, in order to test quantum-critical scaling laws in which the exponent z appears. In some quantities z is the only exponent controlling the asymptotic behavior, while in other quantities the exponent governing the decay of the spin correlation function also enters. By testing for consistent scaling to high precision among several different quantities, we will solidify the claim that conventional quantum-critical scaling applies, with a single well-defined parameter-dependent dynamic exponent and with a universal r^{-2} form of the spin correlations. These calculations are very demanding of computational resources, and we therefore only focus on a single point, $Q = 2$, in the phase diagram of the bimodal random-Q J-Q model. This point is well away from the phase boundary to the Néel phase and should represent the generic behavior with only z varying as we move throughout the RS phase.

We use the stochastic series expansion (SSE) QMC method with efficient loop updates [61,62], which produces exact results within statistical errors. We average all results over more than 10^4 disorder realizations for the final production runs. In

the calculations of finite-T properties, reported below in Secs. III and IV, we start at a relatively high temperature, where the simulation equilibrates easily, and gradually lower T, keeping the disorder realization fixed and continuing the simulation from the last configuration generated at the previous temperature. We accumulate averages of the observables of interest at each temperature on the chosen T grid (in some cases with a varying distance between the T points, as will be described further below). The number of SSE configuration updates performed at each step is large enough to ensure that the system stays in equilibrium and that sufficient statistics can be collected for each disorder realization at each T. Typically we use 10^3 steps for equilibration and 10^3 for accumulating averages at each T. As we will see, the statistical fluctuations of the final disorder-averaged quantities are dominated by the intrinsic sample-to-sample variations, even with this rather modest number of steps per temperature.

To obtain results representing the thermodynamic limit at low temperatures, we need to use very large system sizes, up to $L = 256$, and we anneal down to temperatures as low as $T_0/J = 1/150$ for the largest system size. In the calculations aimed at ground state properties, the temperature has to be much lower in order to avoid finite-temperature effects, and we have only gone up to size $L = 48$ in these calculations.

III. SPECIFIC HEAT

The specific heat C plays an important role in experimental studies of quantum magnetism, providing thermodynamic information about the system. In QMC simulations, the specific heat at low temperatures is in general difficult to compute precisely, as the relative error bars grow when C decreases. We did not consider C in our previous work on the random J-Q model, though it has been computed recently for other variants of the J-Q model and provided experimentally useful benchmark results [63].

To analyze the asymptotic low-T behavior, we have found it better to not compute C directly in the simulations, but to instead analyze the internal energy $E(T)$, which is produced by the SSE method with very high precision even at low T. By fitting a suitable function to $E(T)$, we can deduce the low-temperature properties of the specific heat in the RS phase.

At a quantum-critical point, the specific heat in general scales with temperature as [64]

$$C(T) \propto T^{D/z}, \tag{3}$$

where D is the spatial dimensionality of the system; here $D = 2$. Our hypothesis is that this form, as well as other standard quantum-critical scaling laws [64], holds also inside the RS phase. As already mentioned, our previous work on other quantities showed that $z \geqslant 2$ varies.

From the definition of the specific heat, $C(T) = \partial E(T)/\partial T$, we obtain the expected scaling form of the internal energy $E(T)$ per spin according to Eq. (3),

$$E(T) = E_0 + AT^{D/z+1}, \tag{4}$$

where E_0 is the ground state energy density. We show SSE results for $E(T)$ in Fig. 2(a) for three different system sizes, $L = 32, 64$, and 128. The annealing process used in the simulations started at $T = 0.4$, where the system equilibrates easily
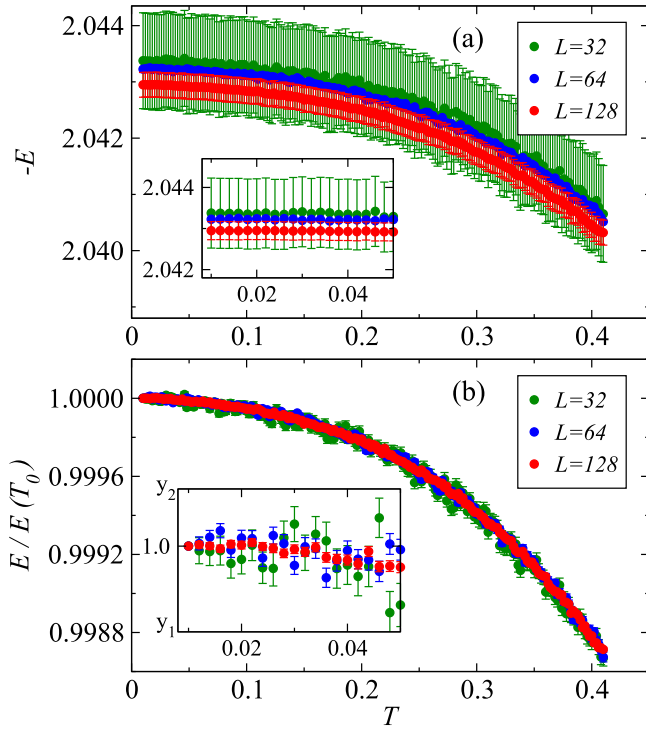
FIG. 2. Internal energy density vs temperature for system sizes $L = 32$, 64, and 128, averaged over 10^3 disorder realizations. The raw data are shown in (a) and the results normalized by $E(T_0)$, with $T_0 = 0.01$, are shown in (b). The insets show magnified graphs of the low-T data. In (a) we do not show the error bars for $L = 64$ in order to avoid clutter (the size of these errors is between those for $L = 32$ and $L = 124$). In the inset of (b), we have marked the lowest and highest points on the vertical axis by $y_1 = 0.99994$ and $y_2 = 1.00004$.

(recall that we set $J = 1$ and report all quantities in units of energy with this convention, and the mean of the bimodal Q value is $\bar{Q} = 2$). Within the error bars we do not observe any finite-size effects, though certainly we do expect some. It can be seen clearly that the errors are highly correlated, with the points for each L forming a curve that is much smoother than what would be expected with independent statistical errors with standard deviation given by the error bars. Clearly, this substantial covariance is due to the fact that the same randomness realizations are used at all temperatures, and the overall fluctuations are primarily due to sample-sample fluctuations.

Since we are only interested in the exponent governing the asymptotic low-temperature form, we write the expected low-T form Eq. (4) as

$$E(T) = E(T_0) + A\left(T^\alpha - T_0^\alpha\right), \tag{5}$$

where T_0 is the lowest temperature studied for a given system size and we have defined the exponent $\alpha = 2/z + 1$. We can then study the behavior of the ratio $E(T)/E(T_0)$, for which we expect the asymptotic form

$$\frac{E(T)}{E(T_0)} = 1 + A_0\left(T^\alpha - T_0^\alpha\right), \tag{6}$$

where now we only have two free parameters; the important exponent α and the unimportant factor A_0. Having eliminated the constant E_0 present before the normalization in Eq. (5) helps to stabilize the results for α in data fits. Moreover, as shown in Fig. 2(b), the error bars of the normalized ratio (computed using bootstrapping) are much smaller, by orders of magnitude, than those of the raw data, and the remaining fluctuations have very little covariance. By definition, the size dependence now should also be much smaller, since all values $E(T)/E(T_0) = 1$ at $T = T_0$ if we use the same T_0 for all system sizes. We do not see any size dependence within the error bars in the temperature window considered in Fig. 2(b), and the remaining error bars after the normalization are smaller for the largest system, due to self-averaging. The number of disorder samples (10^3) and the number of SSE updates for each temperature (10^3 for equilibration and the same number for evaluating expectation values) were identical for all the system sizes in this figure.

In order to confidently study even lower temperatures, for our final analysis we simulated more than 10^4 disorder realizations for system size $L = 256$ down to $T_0 = 1/150$. In order to be able to reach such low temperatures on a fine T grid, while keeping the total time of annealing from the highest to lowest T reasonable, we take the following strategy: After equilibrating a simulation for a given disorder realization at the highest T (here $T = 1$), we decrease T by a constant step ΔT and continue the simulation from the last SSE configuration of the previous temperature. After reaching a certain low T (here $T = 0.1$) where it becomes necessary to decrease the step size, in order to have sufficient resolution to investigate the low-T behavior and also to make sure that equilibrium is properly maintained, we modify the annealing procedure and start to increase the inverse temperature β by a constant step $\Delta\beta$. We thus obtain enough points in the low-T region and the results are reliable.

Based on the above tests for smaller systems with $T_0 = 1/100$, we are confident that the larger system size with the modified annealing procedure gives us results valid as the thermodynamic limit. Normalized results are presented in Fig. 3, with all results up to $T = 1$ shown in Fig. 3(a) and with Fig. 3(b) focusing on the lower temperatures, where, as we will see below, the asymptotic behavior holds without detectable corrections. The error bars are further reduced because of the larger system size and larger number of disorder samples; 10^4 versus 10^3.

When fitting to Eq. (6), the first assumption of course is that T_0 is sufficiently low for the asymptotic behavior to have set in with very small corrections. Even if T_0 is sufficiently low, the corrections will be important above some higher temperature. We therefore carry out fits with data up to a maximum temperature $T_{\max}$ and monitor the goodness of the fit defined as χ^2 per degree of freedom. Figure 4 shows the resulting exponent α versus $T_{\max}$ and also the χ^2 values of the fits. We can clearly observe how the fit gradually improves as $T_{\max}$ is reduced, finally becoming statistically acceptable at $T_{\max} \approx 0.1$. The exponent $\alpha = 2/z + 1$ converges to a value close to 1.5, i.e., the specific heat exponent $2/z \approx 0.5$ in Eq. (3) and $z \approx 4.0$. In the next section we will discuss the scaling behaviors of the uniform susceptibility χ_u and the local susceptibility χ_{loc}, which both should scale with the
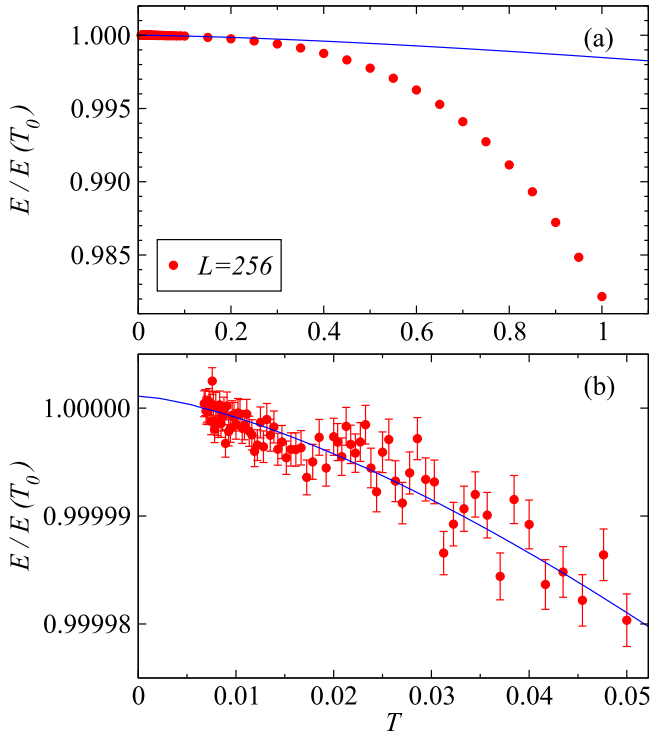
FIG. 3. Normalized energy $E(T)/E(T_0)$ obtained by averaging over more than 10^4 disorder realizations with $L = 256$ and $T_0 = 1/150$. The blue curves show a fit of the data up to $T_{max} = 0.1$ to Eq. (6). The exponent α is graphed versus T_{max} in Fig. 4. Panel (a) shows the whole range of date and (b) focuses on the results for T up to 0.05.

exponent $2/z - 1$. The value of $\alpha = 2/z + 1$ obtained from these quantities is consistent with the value from the specific heat and has smaller error bars, $\alpha = 1.503(6)$. We show this value as the blue line in Fig. 4.
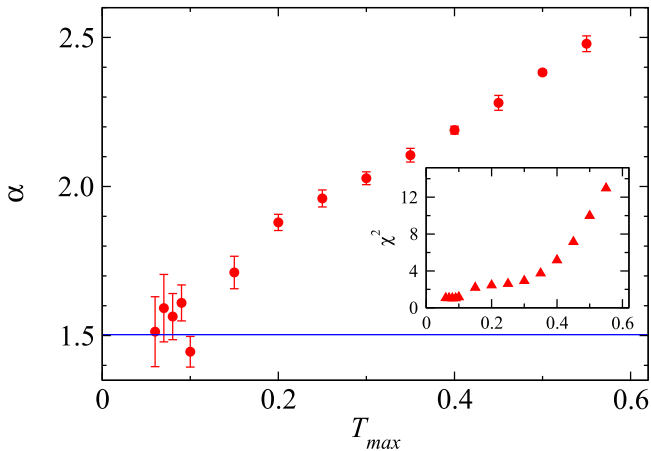

FIG. 4. Exponent $\alpha = 2/z + 1$ in the power law fit, Eq. (6), of the normalized energy as a function of the highest temperature T_{max} included. The data are from Fig. 3. Based on the value of the reduced χ^2 values, which are shown in the inset, the fits are statistically acceptable for $T_{max} \leqslant 0.1$. The result $\alpha = 1.503(6)$ from the susceptibility fits in Sec. IV is shown as the blue line.

IV. SUSCEPTIBILITIES AT FINITE TEMPERATURE

In this section, we focus on the temperature dependence of three different susceptibilities in the thermodynamic limit. As in the previous section, we have studied several different system sizes and in the final analysis used the largest size, $L = 256$, for which our convergence tests show that the results are free from finite-size effects down to the lowest temperatures in the simulations. The data to be presented below are from the same simulations as the energy results in Fig. 3.

The uniform magnetic susceptibility is defined as

$$\chi_u = \frac{1}{TN}\langle m_z^2 \rangle, \tag{7}$$

with the total magnetization

$$m_z = \sum_{i=1}^{N} S_i^z. \tag{8}$$

The local susceptibility at location $\mathbf{x}$ is defined by the Kubo integral

$$\chi_{loc}(\mathbf{x}) = \int_0^{1/T} d\tau \langle S_{\mathbf{x}}^z(\tau)S_{\mathbf{x}}^z(0)\rangle, \tag{9}$$

where $S_{\mathbf{x}}^z(\tau)$ is the standard imaginary-time dependent spin accessible in QMC simulations. In Ref. [48] we showed examples of the local variations in $\chi_{loc}(\mathbf{x})$ and how regions of large response correlate to the presence of spinons and domain walls. Here we will just study the average over $\mathbf{x}$ and refer to this quantity as χ_{loc}. We also calculate the staggered susceptibility defined by the Kubo integral

$$\chi_s = \frac{1}{N}\int_0^{1/T} d\tau \langle m_s(\tau)m_s(0)\rangle, \tag{10}$$

where m_s is the staggered magnetization,

$$m_s = \sum_{i=1}^{N} (-1)^{x_i+y_i} S_i^z. \tag{11}$$

In a quantum critical system in the thermodynamic limit, the low-temperature scaling properties of these observables depend on the dynamic exponent z, and χ_{loc} and χ_s also depend on the exponent η governing the asymptotic correlation function. Following Refs. [64,65], the uniform susceptibility should take the form

$$\chi_u \propto T^{D/z-1}, \tag{12}$$

with $D = 2$. We note that this form is identical to the form of C/T according to Eq. (3).

The local susceptibility, Eq. (9), is the integral of the spin correlation in the imaginary time direction. Translating the results for disordered boson systems by Fisher *et al.* [64] to spins, the mean spin-spin correlations in imaginary time at zero spatial separation should follow the scaling law

$$\langle S_{\mathbf{x}}^z(\tau)S_{\mathbf{x}}^z(0)\rangle \propto \tau^{-(D+z-2+\eta)/z}. \tag{13}$$

Making use of the previous result [48] that the equal-time correlation function $C(r) = \langle S^z(0)S^z(r)\rangle$ scales with distance as r^{-2}, the general critical form $|C(r)| \propto r^{-(D+z-2+\eta)}$ implies the

relationship $\eta = 2 - z$ for the RS state. The time dependence in Eq. (13) then takes the simpler form

$$\left\langle S^z_{\mathbf{x}}(\tau) S^z_{\mathbf{x}}(0) \right\rangle \propto \tau^{-2/z}. \tag{14}$$

The local susceptibility Eq. (9) should then take the following forms depending on the value of z;

$$\chi_{\text{loc}} = \begin{cases} a + b\ln(1/T), & \text{for } z = 2, \\ cT^{2/z-1}, & \text{for } z > 2, \end{cases} \tag{15}$$

with nonuniversal constants a, b, and c. For $z > 2$, this is exactly the same as the common asymptotic form for χ_{u} and C/T. Note again that this form relied on the constraint imposed by the spin correlations decaying as r^{-2}, which can thus be implicitly tested by the local susceptibility. In Ref. [48] we demonstrated the logarithmic $z = 2$ form of Eq. (15) at the phase transition between the Néel and RS states. For the point inside the RS phase studied here, we should only expect the $z > 2$ form.

The staggered susceptibility χ_s is the space-time integral of the staggered correlation function. The often used finite-size scaling version, which we will study in Sec. V, is $\chi_s \propto L^{2-\eta}$, which with the RS relationship $\eta = 2 - z$ becomes $\chi_s \propto L^z$. At $T > 0$ in the thermodynamic limit, the integration cutoff is given by the size $\beta = 1/T$ of the system in the time dimension. Since distances in space (r) and imaginary time (τ) are related to each other in scaling theory by $\tau \propto r^z$, L^z in the finite-size scaling form should be replaced by β when the space dimensions have been effectively taken to infinity. We thus expect

$$\chi_s \propto T^{-1} \tag{16}$$

for the asymptotic form of the staggered susceptibility calculated on a sufficiently large lattice. Thus, because of the specifics of the RS state, this temperature dependent quantity does not allow for an independent test of z, though it implicitly provides a nice way of checking the relationship $\eta = 2 - z$.

We first discuss results for the uniform and local susceptibilities, which both should diverge asymptotically as $T^{-(1-2/z)}$, with $z > 2$. As already noted in Ref. [48], the corrections to the asymptotic form are much larger in χ_{loc} than in χ_{u}. In both quantities, good fits require the use of appropriate scaling corrections, and it was found that a constant added to the divergent form works well with both quantities. We now have data at lower temperatures, and the statistical error are also much improved. The results for the largest system size, $L = 256$, are shown in Fig. 5. Using the form $f(T) = a + bT^{-c}$ to independently fit the two data sets and including only the data points for $\beta = 1/T \geqslant 20$ in the case of χ_{u} and $\beta \geqslant 40$ in the case of χ_{loc}, we obtain the exponents $c = 1 - 2/z = 0.51(2)$ and $0.48(2)$ for χ_{u} and χ_{loc}, respectively. These values are consistent with each other and also with the exponent $\alpha = 2/z + 1 \approx 1.5$ obtained from the specific heat fits in Fig. 4.

To further test the stability of the exponents obtained above, we next include a second correction term in the fitting function, $f(T) = a + bT^{-c} + dT^e$, with which we can obtain statistically sound fits to the two susceptibilities in a much larger range of temperatures; up to the highest temperature $T = 1$ simulated. The fits are shown with red and blue curves in Figs. 5(a) and 5(b), respectively. Even though we now have
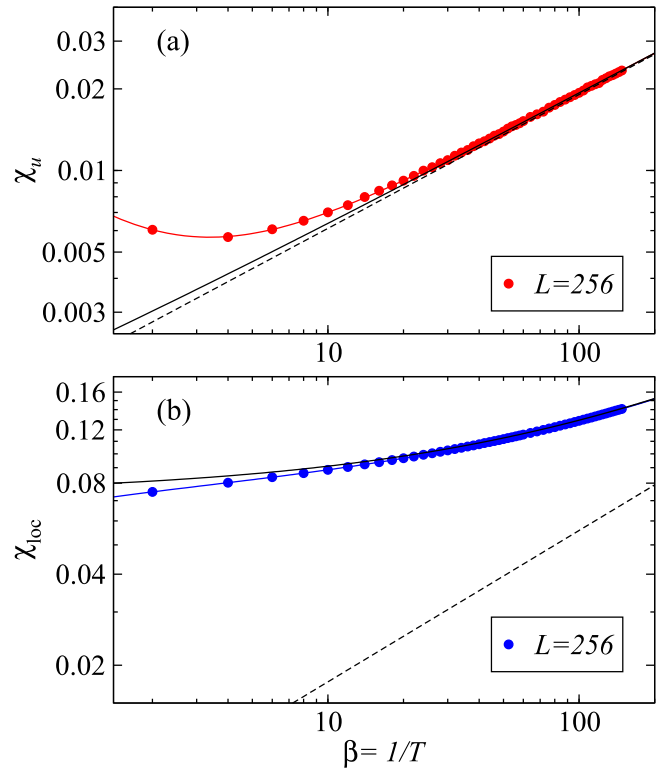

FIG. 5. Temperature dependence of the disorder-averaged uniform (a) and local (b) susceptibility for systems of size $L = 256$. The red and blue curves are fits to the form $f(T) = a + bT^{-c} + dT^e$, where $c = 1 - 2/z > 0$ controls the leading (divergent) behavior. The values of the leading exponents are $c = 0.494(9)$ for χ_{u} and $c = 0.500(8)$ for χ_{loc}. In the correction term the exponent e is positive, with $e = 0.97(6)$ for χ_{u} and $e = 0.60(2)$ for χ_{loc}. The black solid curves show the fitted functions without the second power laws, and the dashed curves show only the leading term bT^{-c}. The error bars on the QMC data are smaller than the graph symbols.

two more free parameters, the larger T range has a net positive effect on the statistical precision of the leading power law in the fit. The exponents obtained are $c = 1 - 2/z = 0.494(9)$ for χ_{u} and $0.500(8)$ for χ_{loc}, which gives us high confidence in the exponents really being the same, and, therefore, that the form r^{-2} of the spin correlation used to constrain the scaling form for χ_{loc} is correct. The correction term $\propto T^e$ has a positive exponent e (given in the caption of Fig. 5) for both quantities.

In Fig. 5 we also show the fitted functions with one or both correction term excluded (i.e., these curves are not from separate fits, but we keep the parameters obtained in the fit to the full function with three terms and just exclude one or two terms). The second power law has only minor effects for $\beta \gtrsim 10$, while the constant term has a very large effect in χ_{loc}. Significant constant contributions can be expected on account of the picture of the RS state consisting of essentially inert VBS domains separated by domain walls and with spinons forming where four domains meet [48]. The constant contributions may stem primarily from the domain walls, while the divergent behavior should originate from the spinons.

Since there is not much statistical covariance between the two susceptibilities in the simulations, we take the average value of the two exponents as the final exponent estimate;
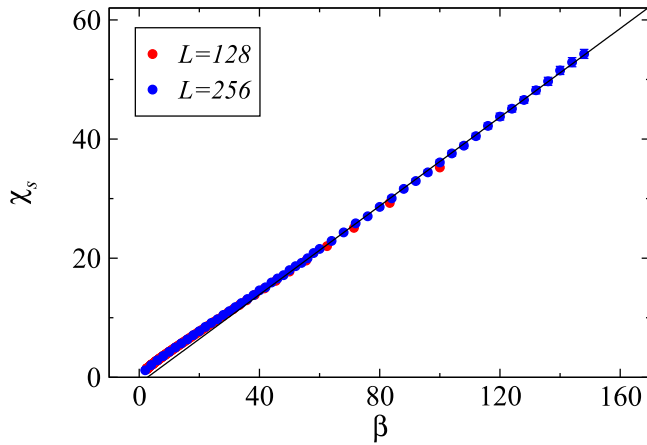
FIG. 6. Dependence of the staggered susceptibility on the inverse temperature for system sizes $L = 128$ and 256. The predicted linear form, Eq. (16), is fully consistent with the data starting from $\beta \approx 50$, as shown with the fitted line.

$1 - 2/z = 0.497(6)$. Then the exponent governing the internal energy, discussed in the previous section, is $\alpha = 2/z + 1 = 1.503(6)$, and this value is indicated with the blue line in Fig. 4. We also note here the data for smaller systems ($L = 64$) and higher temperatures in the previous work [48] gave $1 - 2/z = 0.60(8)$ from the scaling of the uniform susceptibility, which also agrees with our new estimate, though the error bar of the old result is much larger. Our best estimate of α corresponds to the value $z = 3.98(5)$ of the dynamic exponent for the present model parameters.

In Fig. 6 we test the predicted linear form (16) of the staggered susceptibility. We show results for two different system sizes, $L = 128$ and $L = 256$, to illustrate the absence of significant finite size effects up to $\beta = 100$, where we have data for both systems. The further results for $L = 256$ up to $\beta = 150$ continue with the same linear trend and there is no reason to suspect significant size effects here. The results from $\beta = 50$ to 150 are fully consistent with the linear form. This perfect agreement with the predicted form strongly supports the relationship $\eta = 2 - z$ and the r^{-2} form of the equal-time correlation function.

V. GROUND STATE FINITE-SIZE SCALING

It is also useful to study systems at sufficiently low temperatures for computed quantities to have converged to their ground state values. The dynamic exponent $z \approx 4.0$ estimated from the scaling behaviors analyzed in the previous sections also controls the finite-size excitation gaps in the system; we expect the smallest gap to scale as $\Delta \propto L^{-z}$. Asymptotically, for large systems we therefore have to reach down to temperatures of order L^{-z} to converge to the ground state. However, as we will show below, the gaps also have corrections that corresponds to an effective, size-dependent dynamic exponent z_{eff} that is smaller than z for small systems (and we will extrapolate for the asymptotic value z). Moreover, in principle we can use temperatures of the form $T(L) = aL^{-b}$ with any exponent $b > 0$ and still reach the ground state up to some system size if the proportionality factor a is small enough.

We have carried out simulations at $T = aL^{-2}$ with different prefactors a to test the convergence and found that all results are well converged to the ground state with $a = 1$ up to $L = 48$. Our aim here is to use the size dependence of appropriate ground state quantities to obtain an independent estimate of the dynamic exponent and also to further test the r^{-2} form of the spin correlation function.

An often used method to test the scaling of the gap without accessing any excited states directly is to compute the static structure factor $S(\mathbf{q})$ and the corresponding static susceptibility $\chi(\mathbf{q})$ at the wave vector $\mathbf{q}$ of interest. The ratio $\Delta^*(q) = 2S(\mathbf{q})/\chi(\mathbf{q})$ is an upper bound to the true gap, $\Delta(\mathbf{q}) \leqslant \Delta^*(\mathbf{q})$. The bound is derived from sum rules for the dynamic structure factor and is exact for a single mode. In general, the bound may not be very good quantitatively, but for a critical mode Δ^* is expected to have the same asymptotic scaling properties as the gap. We refer to Ref. [27] for more details on this approach and an application to another disordered spin system. We will investigate the scaling properties of the ratio $\chi(\mathbf{Q})/S(\mathbf{Q})$, where $\mathbf{Q}$ is the antiferromagnetic wave vector.

The static structure factor is just the Fourier transform of the spin correlation function,

$$S(\mathbf{q}) = \sum_{\mathbf{r}} e^{-i\mathbf{q}\cdot\mathbf{r}} \langle S^z(0)S^z(\mathbf{r}) \rangle. \tag{17}$$

We set $\mathbf{q} = (\pi, \pi)$ and name this structure factor $S(\pi)$. If the spin correlations decay as r^{-2} in the RS state, we expect the asymptotic size dependence to be

$$S(\pi) = a + b\ln(L). \tag{18}$$

The corresponding staggered susceptibility $\chi_s = \chi(\mathbf{Q})$ was already defined in Eq. (10) and we mentioned its expected finite-size scaling form when the relationship $\eta = 2 - z$ is imposed;

$$\chi_s \propto L^z. \tag{19}$$

As mentioned above, for a critical mode $\chi(\mathbf{Q})/S(\mathbf{Q})$ is normally expected to scale as L^z, but in the case at hand here there is a logarithmic correction, due to Eq. (18) because of the r^{-2} decay in two dimensions. We will nevertheless investigate the ratio $\chi_s/S(\pi)$ and attempt to extract z from its leading asymptotic L^z form. In addition, we can also extract z from just the divergence of χ_s, which is not affected by the logarithmic correction.

In Fig. 7 we graph the size dependence of $S(\pi)$, χ_s, and $\chi_s/S(\pi)$ on a log-log scale. In the case of $S(\pi)$, the behavior looks almost constant in the main graph, but when zooming in (the inset of Fig. 7) and graphing on a log-linear scale, the expected logarithmic divergence is apparent. Both χ_s and $\chi_s/S(\pi)$ diverge strongly, but we do not observe any clear power-law behaviors. The upward curvature on the log-log plot implies that the effective dynamic exponent z_{eff} increases with increasing system size, and corrections to scaling must be considered for the available system sizes in order to extract the asymptotic value $z_{\text{eff}}(L \to \infty) \to z$. Fitting to two power laws (the curves shown in Fig. 7) give $z = 3.7(3)$ from χ_s and $z = 3.5(4)$ from $\chi_s/S(\pi)$ from the leading terms $\propto L^z$. Here the result from χ_s should be more reliable, because of the logarithmic corrections expected in the ratio $\chi_s/S(\pi)$.
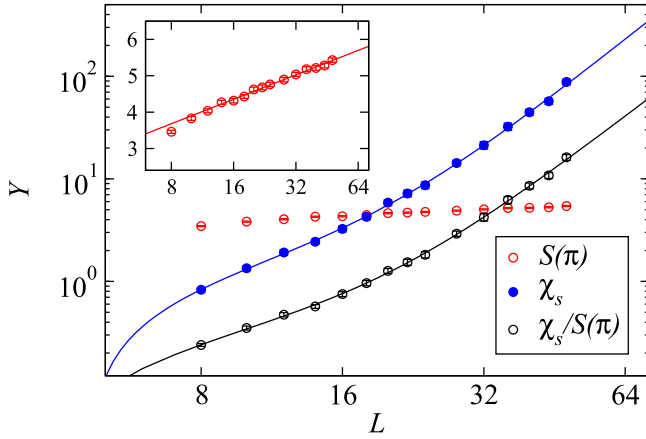
FIG. 7. Log-log plot showing the size dependence of $S(\pi)$, χ_s, and $\chi_s/S(\pi)$ for system sizes up to $L = 48$. The blue and black curves show fits to the form $Y = aL^z + bL^c$. The inset shows a log-linear plot of $S(\pi)$, making clear the logarithmic divergence of the form Eq. (18), shown by the fitted line.

Because of the relatively large error bars, it is not possible to explicitly observe the multiplicative logarithm in the ratio, though we see it in $S(\pi)$ when analyzed separately.

We also can define an effective dynamic exponent z_{eff} for a pair of systems with sizes L and $2L$,

$$z_{\text{eff}}(L_{\text{eff}}) = \frac{1}{\ln(2)}[\ln(Y_{2L}) - \ln(Y_L)], \qquad (20)$$

where the effective system size can be defined as $L_{\text{eff}} = (2L^2)^{1/2}$ (though we could also just use L as the size). Y stands for one of the two observables; χ_s or $\chi_s/S(\pi)$. As shown in Fig. 8, both of these two effective exponents converge to
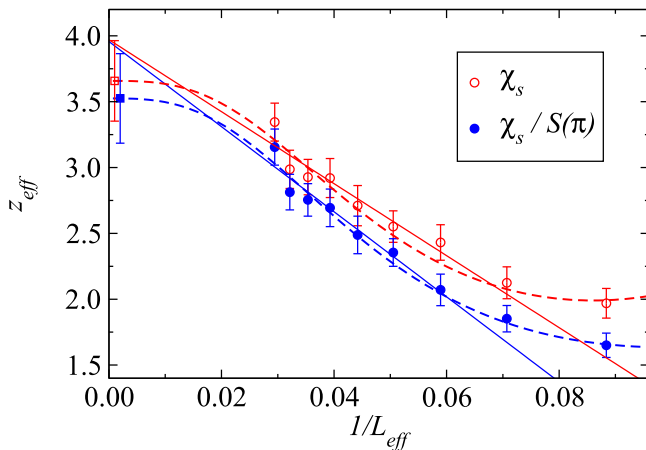

FIG. 8. Effective dynamic exponent defined using two system sizes, L and $2L$, according to Eq. (20) for the quantities χ_s (red symbols) and $\chi_s/S(\pi)$ (blue symbols). The effective system size is defined as $L_{\text{eff}} = (2L^2)^{1/2}$. The solid lines show linear fits in $1/L_{\text{eff}}$ giving the estimates of the extrapolated exponents $z = z_{\text{eff}}(L \to \infty) = 3.96(17)$ from χ_s and $z = 3.94(14)$ from $\chi_s/S(\pi)$ the text. The dashed curves are obtained from the direct fits of the size dependent quantities in Fig. 7 to a form with two power laws, which were subsequently used in Eq. (20). The resulting extrapolated dynamic exponent with error bars are indicated close to $1/L_{\text{eff}} = 0$.

the same value, $z \approx 4$, approximately linearly with $1/L_{\text{eff}}$ as system size grows. Linear fits of the form $z_{\text{eff}} = z + c/L_{\text{eff}}$ with the data starting from $L_{\text{eff}} > 16$ (below which there are clearly large corrections) give $z = 3.96(17)$ from χ_s and $z = 3.94(14)$ from $\chi_s/S(\pi)$, both in full agreement with our best determination of the dynamic exponent, $z = 3.98(5)$, in the previous section. The results also agree with those from the direct fits to the size dependent quantities in Fig. 7, but the latter have much larger error bars. Clearly, the smaller errors when fitting to z_{eff} is due to the assumed linear behavior when fitting the data in Fig. 8. The inferred size dependent z_{eff} based on the fits in Fig. 7 is also shown in Fig. 8. The shapes of the curves here are not certain, as is also reflected in the large error bars on the extrapolated z values, because of the large uncertainty in the correction exponent in the two-power fits in Fig. 7.

VI. CONCLUSION AND DISCUSSION

We have studied the properties of the RS state in the 2D random-Q J-Q model, using large-scale QMC simulations to test low-temperature critical scaling forms in the thermodynamic limit as well as finite-size scaling forms in the ground state. A salient feature of the RS state is that the spin-spin correlations at $T = 0$ decay with distance as r^{-2}. Formally, the exponent 2 implies the relationship $\eta = 2 - z$ in standard quantum-critical scaling forms. Quantities that do not involve η, such as the uniform and local susceptibilities, exhibit low-temperature behaviors expected in critical systems [64] with a common value of the dynamic exponent z. Quantities with scaling forms involving η are fully consistent with $\eta = 2 - z$ with the same z as that extracted from the other quantities. The high-precision calculations reported here for a single point inside the RS phase, in combination with the less precise results for several points in Ref. [48], establish beyond a reasonable doubt that the RS phase in the J-Q model corresponds to a finite-disorder critical RG fixed point, with universal r^{-2} decay of the spin correlations and varying dynamic exponent $z \geqslant 2$.

Below, in Sec. VI A we provide some further comments on the term "2D RS state" as it compares to the well known 1D counterpart. In Sec. VI B we discuss the possible generality of the RS state characterized here and how our findings fit into related scenarios for randomness-induced states proposed within other approaches. In Sec. VI C we discuss potential experimental realizations of RS states and promising avenues to further investigate candidate materials.

A. On the RS state terminology

The 1D RS state is an IRFP, and one may then ask whether the term 2D RS state is even appropriate for the finite-disorder fixed point we have established here. Presumably, the RS term was coined to describe the end result of the SDRG method, which is a single valence-bond configuration with a characteristic distribution of the length of the bonds [7,8]. This single configuration is of course only a caricature of the actual superposition ground state of a system such as the $S = 1/2$ Heisenberg chain with random couplings, but it still captures the asymptotic properties correctly in one dimension [9] (perhaps up to logarithmic corrections that have been

discussed recently [13]). In other words, the SDRG method produces a typical valence bond configuration drawn from the true ground state.

The typicality aspect of the SDRG method and the RS state is closely connected to the IRFP nature of the fixed point. Conversely, one might not expect the SDRG method applied to 2D systems with finite-disorder fixed points to produce completely representative results of the true ground state, which is just another way of saying that the SDRG method is reliable only when it flows to an IRFP. It has still been argued that useful approximations can be obtained. For instance, in the early work by Bhatt and Lee [10], the logarithmic width of the coupling distribution was found to not grow under the SDRG procedure in the case of 2D dilute randomly located moments, and the susceptibility was found to diverge as $T^{-\alpha}$ with $\alpha < 1$. These are not signatures of an IRFP, and the latter behavior can be interpreted as a finite value of the dynamic exponent z according to Eq. (12). Nevertheless, the SDRG method produced a set of frozen singlets, e.g., an RS state, and the results are believed to capture the essential physics of the system studied.

We have here not discussed the microscopic mechanisms underlying the RS state, which were described in detail in Ref. [48], and also within a different theoretical framework in Ref. [47]. The essence is that the mechanism of interacting spinons in a background of VBS domains is a close analogy to the 1D case. The analogy is the closest when the 1D RS state is constructed starting from a spontaneously dimerized system (e.g., the J-Q chain for large Q/J) [13], instead of a critical system like the standard Heisenberg chain. Then one can really identify out-of-phase dimerized chain segments separated by localized spinons, and these spinons produce an RS state through interactions mediated by the gapped host segments. Similarly, when starting from the VBS ordered 2D J-Q model, localized spinons induced by randomness can be identified which appear pairwise and interact with each other mainly through the domain walls [48] and form a critical state. It is not clear why the spin correlations in this state decay as r^{-2}, which is also the form in the 1D RS state, but a power-law decay in any case is a manifestation of physics similar to the 1D RS state.

In the system studied in the present paper, the dynamic exponent $z \approx 4$ and it was previously shown that it can grow much larger—up to $z \approx 7$ was found at points deeper inside the RS phase in Ref. [48] (and there is likely no upper bound in principle if other suitable interactions are considered). Thus, the system can exhibit slow dynamics. With the imposed exponent relation $\eta = 2 - z$, we found that the onsite (imaginary time) dynamic spin-spin correlation function takes the asymptotic form $\langle \mathbf{S}_i(\tau)\mathbf{S}_i(0)\rangle \propto \tau^{-2/z}$, representing a slow decay when z becomes large. Here it should be noted that the slow dynamics should correspond to weak effective couplings between spins in long valence bonds, in analogy with the 1D RS state where the logarithmic form of the asymptotic decay of the correlations originates from rare very long bonds. Thus, while the finite-z 2D state does not have the extreme slow dynamics of the 1D RS system, it can still approach that behavior when z becomes large, and for the same physical reasons.

Given all the above reasoning, the term 2D RS state for the critical phase in the random J-Q model appears appropriate,

despite the fact that it does not correspond to an IRFP. It is not even clear whether an IRFP exists in SU(2) spin models with realistic short-range interactions, given the many negative results based on the SDRG method [10,15–20,52]. These studies have also found finite-disorder fixed points, though they were not characterized in the kind of detail achieved here, e.g., as regards the r^{-2} form of the spin correlations.

Finally, with regards to terminology, we note that Griffiths phases [66] are gapless phases of random systems appearing in the neighborhood of transitions into ordered phases. However, physics involved in the formation of a quantum Griffiths phase is quite different from the mechanisms underlying the RS state. The gapless behaviors arise from rare, arbitrarily large ordered clusters within an otherwise gapped bulk. Such ordered clusters do not appear in the RS phase, where the critical properties are intrinsic to the network of interacting spinons. The differences are well illustrated by dilute magnetic semiconductors, where random antiferromagnetic interactions lead to RS physics [10], and there is not necessarily any ordered phase close by which spawns the RS state. In contrast, in the neighborhood of a ferromagnetic transition, a Griffiths phase with completely different properties arises [67] due to the presence of large ferromagnetic clusters. The properties of Griffiths phases in general depend sensitively on the nearby phases which it is a mixture of. A quantum Griffiths phase has been discussed in the content of spin ice, where the classical ice state changes character in the presence of strong quantum fluctuations and becomes a Griffiths phase (referred to as a disorder-induced spin liquid), located in parameter space between a paramagnetic phase and a Coulomb spin liquid [68]. Again, this Griffiths phase is very different from the RS phase. The RS state with very specific properties discussed here should not be confused with a generic Griffiths state.

B. Generality of the 2D RS state

While we have not proved that the RS state studied here is also generic beyond the "designer" interactions of the J-Q model, there is mounting evidence for this being the case. Recently, a DMRG study [46] of the square-lattice $S = 1/2$ Heisenberg model with random frustrated bonds detected spin correlation functions apparently decaying with the same power-law r^{-2} as in the random J-Q model. The systems accessible with DMRG, beyond the very small lattice accessible with the ED method [35,38–45], are still not very large and the associated finite-T properties of the system have not been studied yet. It should be possible to reach larger systems with the DMRG method in the future, and progress has also been made on $T > 0$ properties [69].

From the physical perspective, Kimchi _et al._ [47] also proposed that the mechanism causing the RS state in frustrated quantum magnets should be VBS domains with topological defects carrying spinons, exactly as found in the random J-Q model [48]. If indeed the physical ingredients are the same, and the spinons in the J-Q model do not form antiferromagnetic long-range order (which was proposed [47] but has not been observed), then there is no strong reason why frustrated interactions (in the conventional sense of inability to satisfy antiferromagnetic spin orientations along any loop on the

lattice) should cause a low-energy state different from that resulting from the different forms of competing interactions of the J-Q model. In a recent work, Dey and Vojta [55] also made a similar remark in the context of a semiclassical analysis of spin glasses in weakly frustrated 2D systems, suggesting that strong quantum effects should induce local VBS formation and transform the quasiclassical spin glass into the proposed RS state [47,48]. This picture as well does not appear to depend on what microscopic interactions cause the VBS domains.

Kimchi *et al.* [47] also speculated that the RS state in the frustrated systems may only be an intermediate-energy state, which could be unstable to formation of a spin glass at the lowest energies. As we discussed in Sec. I A, to our knowledge there are no concrete reliable calculations showing that a spin glass state is even possible in 2D $S = 1/2$ systems with short-range interactions. Instead, the RS state may be what generically replaces a classical or semiclassical spin glass when the quantum fluctuations are strong—this is also the picture discussed by Dey and Vojta [55].

Numerically we can in principle not completely rule out that the RS state we have characterized is unstable to anti-ferromagnetic order at even lower temperatures than we have reached. However, the ordering scenario appears implausible based on the consistent power-law scaling observed for all the quantities studied, down to what already is a very low temperature scale (of the order 10^{-2} of the microscopic coupling scale). In contrast, Kimchi *et al.* [47] did not even discuss the possibility of an intermediate RS flow in systems without conventional frustration, implicitly assuming that the ordering tendency is strong unless frustrated interactions are present. At the very least, it is now clear that the RS state we have characterized exists over a vast range of length and energy scales, and it must correspond to an RG fixed point of random 2D quantum magnets.

To better connect the picture of the frustrated RS state to SDRG calculations and the prototypical RS state of the J-Q model, it would be useful to study the dynamic exponent within the SDRG scheme. Normally, the results of SDRG calculations are expressed in terms of an exponent γ, which controls the low-temperature specific heat C/T and susceptibility χ_u; they both scale as $T^{-\gamma}$ with $\gamma < 1$ [10,52]. In our picture, where the scaling is conventional quantum-critical scaling with the constraint $\eta = 2 - z$ (which is important when considering the local susceptibility χ_{loc}, which attains the same divergence as χ_u and C/T only if $\eta = 2 - z$), the exponent is expressed as $\gamma = 1 - 2/z$. It would be interesting to extract the dynamic exponent in the SDRG procedure and test this relationship (which we believe must apply). It would of course also be interesting to check the decay form of the spin-spin correlations within the SDRG framework, but unfortunately it is difficult to extract real-space information from the decimation procedure in more than one dimension. As far as we are aware, this has never been done.

C. Experiments

Many of the quantities we have studied here can be tested experimentally. The perhaps most fundamental and definite aspect of the RS state characterized here is the r^{-2} decay of the spin correlations in the ground state. In principle this form can be tested by inelastic neutron scattering through the associated logarithmic divergence of the static structure factor $S(\mathbf{q})$ in the limit $\mathbf{q} \to (\pi, \pi)$. The static structure factor is obtained by integrating the dynamic structure factor $S(\mathbf{q}, \omega)$ over ω, but clearly the logarithmic divergence will not be easy to detect, given typical experimental resolution, temperature effects, and impurity effects not corresponding solely to random couplings. Nevertheless, it may be useful to look for a possible anomalous shape of the peak of $S(\mathbf{q})$ versus $\mathbf{q}$ in candidate RS materials. The predicted linear dependence on T^{-1} of the staggered susceptibility, Eq. (16), may be more practical for tests with inelastic neutron scattering than $S(\pi, \pi)$; it can be obtained from the ω^{-1}-weighted frequency integral of $S(\mathbf{q}, \omega)$ at $\mathbf{q} = (\pi, \pi)$.

The specific heat and the uniform magnetic susceptibility are more easily accessible than dynamic quantities, but both may also be sensitive to effects beyond the disorder giving rise to the RS state. In particular, impurity moments in addition to random couplings should lead to other contributions to the susceptibility, though anomalous, non-Curie behaviors may still apply [70].

In our previous work [48], we pointed out that $Sr_2CuTe_{1-x}W_xO_6$, which for $x = 0$ is a good realization of the square-lattice $S = 1/2$ Heisenberg model [71,72], is a promising candidate for RS physics. For W fractions $0 < x < 1$, the system is randomly frustrated, with first- and second-neighbor Heisenberg couplings mediated by plaquette-centered Te or W ions, respectively. The system has columnar antiferromagnetic order for $x \gtrsim 0.7$ [73,74] but no order for $0.1 \lesssim x \lesssim 0.7$ [75,76]. Though a Curie tail was reported in the susceptibility [76], the data at low temperatures can actually be better fitted to a power law $\chi_u \propto T^{-\gamma}$ with $\gamma \approx 0.7$ (weakly dependent on x in the range where there is no magnetic order) [48]. On one hand this behavior may indicate an RS phase, but on the other hand the specific heat does not show the same power law $C/T \propto T^{-\gamma}$ that we have demonstrated here (and which holds also within the SDRG method [52]); instead a shoulder anomaly is present in C/T near 1.2 K, followed at lower temperatures by a drop more rapid than the expected power law [76]. It is not clear, however, what role subtraction of claimed impurity contributions play here, as those "impurities" may at least partially be the spinons of the RS state. Thus, the baby may have been thrown out with the bath water. Further specific heat studies will be important.

Kimchi *et al.* suggested that $YbMgGaO_4$ is a likely RS system [47]. This material had previously been regarded as quantum spin liquid [53] and later as a spin glass [54]. Indeed the material exhibits a power-law decay of the specific heat and a divergent susceptibility [53,54]. While the former is natural under some scenarios in spin liquids, the divergent susceptibility is not. The divergent susceptibility was previously attributed to magnetic impurities not part of the collective bulk state [77]. It would be interesting to further analyze the exponents and test whether the specific heat and the susceptibility are mutually consistent in the way tested here for the J-Q model.

A strong case for RS physics in $LiZn_2Mo_3O_8$ and related materials was made by Kimchi *et al.* [52], primarily based on the behavior of the system in a magnetic field and scaling

forms obtained from the SDRG scheme and related considerations. We have not yet studied the random J-Q model in a magnetic field, but such calculations are possible [78,79] and would be interesting to carry out in the future. $LiZn_2Mo_3O_8$ had previously been proposed to realize a VBS state with 1/3 of the spins remaining paramagnetic and subject to weak antiferromagnetic couplings [80]. Kimchi *et al.* [52] also proposed that $H_3LiIr_2O_6$ may realize the RS phase. At zero field, both C/T and χ_u have a low-temperature form $T^{-\gamma}$ with $\gamma \approx 0.5$ [81], and this behavior was originally attributed to a low density of spin defects in a bulk quantum spin liquid. A complication with $LiZn_2Mo_3O_8$ and $H_3LiIr_2O_6$ is strong Dzyaloshinskii-Moriya interactions, which was taken into account in the treatment by Kimchi *et al.* [52]. It is not clear whether the RS state as realized in the J-Q model can capture all aspects of random quantum magnets when additional effects, e.g., Dzyaloshinskii-Moriya interactions, are important. However, if the system still remains critical with finite dynamic exponent the general scaling laws tested here should still hold, though not necessarily with the $\eta = 2 - z$ constraint.

Finally, we mention α-$Ru_{1-x}Ir_xCl_3$, which recently has attracted attention as a possible randomness-induced spin liquid [82–84] or RS state [85] when x slightly exceeds 0.2. While various power-law behaviors have been observed, the exponents governing χ_u and C/T are distinctly different, and therefore the state appears to be quite different from the conventional RS state. One possible explanation for the violations is that the system has both bond disorder and spin vacancies. In the J-Q model, vacancies induce long-range antiferromagnetic order because the spinon pairing imposed by the topological defects can no longer be strictly maintained when the moments associated with vacancies are completely randomly distributed [48]. It is possible that some power-law scaling can still be observed in some range of temperatures,

and in principle this can be tested within the J-Q model, for which the previous work only established that some long-range order is induced by vacancies. This long-range order can in principle be destroyed in the presence of frustrated interactions, and then an RS state may still form. The effects of vacancies in a frustrated triangular-lattice quantum magnet were theoretically studied by Riedl *et al.* [70], but no concrete predictions for thermodynamics were presented. It would be interesting to further study the interplay of vacancies and coupling disorder.

Note added. In a recent collaboration with experimental groups using neutron diffraction and μSR techniques on $Sr_2CuTe_{1-x}W_xO_6$ [86], we have demonstrated that the Néel order in this material vanishes already at $x \approx 0.03$ (i.e., well below the previously estimated critical W fraction $x \approx 0.1$ [75,76]) and that the properties of the disordered phase agree with our RS scenario. The dynamic exponent extracted from the μSR relaxation rate slightly exceeds the lower RS bound $z = 2$ at $x = 0.05$ (close to the transition from the Néel state) and grows to a value $z > 3$ at $x = 0.1$ (deeper inside the RS phase). The neutron diffraction measurements show significant short-range Néel-type spin correlations throughout the disordered phase, as expected on account of the $1/r^2$ staggered spin correlations in the RS phase.

[1] P. W. Anderson, Absence of diffusion in certain random lattices, Phys. Rev. **109**, 1492 (1958).

[2] L. Fleishman and P. W. Anderson, Interactions and the Anderson transition, Phys. Rev. B **21**, 2366 (1980).

[3] B. L. Altshuler, Y. Gefen, A. Kamenev, and L. S. Levitov, Quasiparticle Lifetime in a Finite System: A Nonperturbative Approach, Phys. Rev. Lett. **78**, 2803 (1997).

[4] D. M. Basko, I. L. Aleiner, and B. L. Altshuler, Metal-insulator transition in a weakly interacting many-electron system with localized single-particle states, Ann. Phys. **321**, 1126 (2006)

[5] I. V. Gornyi, A. D. Mirlin, and D. G. Polyakov, Interacting Electrons in Disordered Wires: Anderson Localization and Low-T Transport, Phys. Rev. Lett. **95**, 206603 (2005).

[6] A. Pal and D. A. Huse, Many-body localization phase transition, Phys. Rev. B **82**, 174411 (2010).

[7] S. K. Ma, C. Dasgupta, and C.-K. Hu, Random Antiferromagnetic Chain, Phys. Rev. Lett. **43**, 1434 (1979).

[8] C. Dasgupta and S. K. Ma, Low-temperature properties of the random Heisenberg antiferromagnetic chain, Phys. Rev. B **22**, 1305 (1980).

[9] D. S. Fisher, Random antiferromagnetic quantum spin chains, Phys. Rev. B **50**, 3799 (1994).

[10] R. N. Bhatt and P. A. Lee, Scaling Studies of Highly Disordered Spin-1/2 Antiferromagnetic Systems, Phys. Rev. Lett. **48**, 344 (1982).

[11] R. A. Hyman and K. Yang, Impurity Driven Phase Transition in the Antiferromagnetic Spin-1 Chain, Phys. Rev. Lett. **78**, 1783 (1997).

[12] A. Lavarélo and G. Roux, Localization of Spinons in Random Majumdar-Ghosh Chains, Phys. Rev. Lett. **110**, 087204 (2013).

[13] Y.-R. Shu, D.-X. Yao, C.-W. Ke, Y.-C. Lin, and A. W. Sandvik, Properties of the random-singlet phase: From the disordered Heisenberg chain to an amorphous valence-bond solid, Phys. Rev. B **94**, 174442 (2016).

[14] I. A. Kovács and Ferenc Iglói, Renormalization group study of the two-dimensional random transverse-field Ising model, Phys. Rev. B **82**, 054437 (2010).

[15] R. Mélin, Antiferromagnetism in a doped spin-Peierls model: Classical and quantum behaviors, Eur. Phys. J. B **16**, 261 (2000).

[16] K. Damle, O. Motrunich, and D. A. Huse, Dynamics and Transport in Random Antiferromagnetic Spin Chains, Phys. Rev. Lett. **84**, 3434 (2000).

[17] O. Motrunich, S.-C. Mau, D. A. Huse, and D. S. Fisher, Infinite-randomness quantum ising critical fixed points, Phys. Rev. B **61**, 1160 (2000).

[18] Y.-C. Lin, R. Mélin, H. Rieger, and F. Iglói, Low-energy fixed points of random Heisenberg models, Phys. Rev. B **68**, 024424 (2003).

[19] Y.-C. Lin, H. Rieger, N. Laflorencie, and F. Iglói, Strong-disorder renormalization group study of $S = \frac{1}{2}$ Heisenberg antiferromagnet layers and bilayers with bond randomness, site dilution, and dimer dilution, Phys. Rev. B **74**, 024427 (2006).

[20] C. R. Laumman, D. A. Huse, A. W. W. Ludwing, G. Refael, S. Trebst, and M. Troyer, Strong-disorder renormalization for interacting non-Abelian anyon systems in two dimensions, Phys. Rev. B **85**, 224201 (2012).

[21] N. Laflorencie, S. Wessel, A. Läuchli, and H. Rieger, Random-exchange quantum Heisenberg antiferromagnets on a square lattice, Phys. Rev. B **73**, 060403(R) (2006).

[22] A. W. Sandvik, Classical percolation transition in the diluted two-dimensional S=1/2 Heisenberg antiferromagnet, Phys. Rev. B **66**, 024418 (2002).

[23] A. W. Sandvik, Multicritical Point in a Diluted Bilayer Heisenberg Quantum Antiferromagnet, Phys. Rev. Lett. **89**, 177201 (2002).

[24] O. P. Vajk and M. Greven, Quantum Versus Geometric Disorder in a Two-Dimensional Heisenberg Antiferromagnet, Phys. Rev. Lett. **89**, 177202 (2002).

[25] R. Yu, T. Roscilde, and S. Haas, Quantum Percolation in Two-Dimensional Antiferromagnets, Phys. Rev. Lett. **94**, 197204 (2005).

[26] A. W. Sandvik, Quantum Criticality and Percolation in Dimer-Diluted Two-Dimensional Antiferromagnets, Phys. Rev. Lett. **96**, 207201 (2006).

[27] L. Wang and A. W. Sandvik, Low-energy excitations of two-dimensional diluted Heisenberg quantum antiferromagnets, Phys. Rev. B **81**, 054417 (2010).

[28] N. Ma, A. W. Sandvik, and D.-X. Yao, Mott glass phase in a diluted bilayer Heisenberg quantum antiferromagnet, J. Phys.: Conf. Ser. **640**, 012045 (2015).

[29] S. Iyer, D. Pekker, and G. Refael, Mott glass to superfluid transition for random bosons in two dimensions, Phys. Rev. B **85**, 094202 (2012).

[30] A. J. Bray and M. A. Moore, Replica theory of quantum spin glasses, J. Phys. C **13**, L655 (1980).

[31] K. D. Usadel, Spin glass transition in an Ising spin system with transverse field, Solid State Commun. **58**, 629 (1986).

[32] H. Rieger and A. P. Young, Zero-Temperature Quantum Phase Transition of a Two-Dimensional Ising Spin Glass, Phys. Rev. Lett. **72**, 4141 (1994).

[33] S. Sachdev and J. Ye, Gapless Spin-Fluid Ground State in a Random Quantum Heisenberg Magnet, Phys. Rev. Lett. **70**, 3339 (1993).

[34] N. Read, Subir Sachdev, and J. Ye, Landau theory of quantum spin glasses of rotors and Ising spins, Phys. Rev. B **52**, 384 (1995).

[35] J. Oitmaa and O. P. Sushkov, Two-Dimensional Randomly Frustrated Spin-1/2 Heisenberg Model, Phys. Rev. Lett. **87**, 167206 (2001).

[36] M. Tarzia and G. Biroli, The valence bond glass phase, Europhys. Lett. **82**, 67008 (2008).

[37] R. R. P. Singh, Valence Bond Glass Phase in Dilute Kagome Antiferromagnets, Phys. Rev. Lett. **104**, 177203 (2010).

[38] K. Watanabe, H. Kawamura, H. Nakano, and T. Sakai, Quantum spin-liquid behavior in the spin-1/2 random Heisenberg antiferromagnet on the triangular lattice, J. Phys. Soc. Jpn. **83**, 034714 (2014).

[39] H. Kawamura, K. Watanabe, and T. Shimokawa, Quantum spin-liquid behavior in the spin-1/2 random-bond Heisenberg antiferromagnet on the kagome lattice, J. Phys. Soc. Jpn. **83**, 103704 (2014).

[40] T. Shimokawa, K. Watanabe, and H. Kawamura, Static and dynamical spin correlations of the $S = 1/2$ random-bond antiferromagnetic Heisenberg model on the triangular and kagome lattices, Phys. Rev. B **92**, 134407 (2015).

[41] K. Uematsu and H. Kawamura, Randomness-Induced quantum spin liquid behavior in the $s = 1/2$ random $J_1 - J_2$ Heisenberg antiferromagnet on the honeycomb lattice, J. Phys. Soc. Jpn. **86**, 044704 (2017).

[42] K. Uematsu and H. Kawamura, Randomness-induced quantum spin liquid behavior in the $s = 1/2$ random $J_1 - J_2$ Heisenberg antiferromagnet on the square lattice, Phys. Rev. B **98**, 134427 (2018).

[43] H. Kawamura and K. Uematsu, Nature of the randomness-induced quantum spin liquids in two dimensions, J. Phys.: Condens. Matter **31**, 504003 (2019).

[44] K. Uematsu and H. Kawamura, Randomness-induced Quantum Spin Liquid Behavior in the $s = 1/2$ Random-Bond Heisenberg Antiferromagnet on the Pyrochlore Lattice, Phys. Rev. Lett. **123**, 087201 (2019).

[45] H.-Q. Wu, S.-S. Gong, and D. N. Sheng, Randomness-induced spin-liquid-like phase in the spin-$\frac{1}{2}$ $J_1 - J_2$ triangular Heisenberg model, Phys. Rev. B **99**, 085141 (2019).

[46] H.-D. Ren, T.-Y. Xiong, H.-Q. Wu, D. N. Sheng, and S.-S. Gong, Characterizing random-singlet state in two-dimensional frustrated quantum magnets and implications for the double perovskite $Sr_2CuTe_{1-x}W_xO_6$, arXiv:2004.02128.

[47] I. Kimchi, A. Nahum, and T. Senthil, Valance Bonds in Random Quantum Magnets: Theory and Application to $YbMgGaO_4$, Phys. Rev. X **8**, 031028 (2018).

[48] L. Liu, H. Shao, Y.-C. Lin, W. Guo, and A. W. Sandvik, Random-Singlet Phase in Disordered Two-Dimensional Quantum Magnets, Phys. Rev. X **8**, 041040 (2018).

[49] Y. Imry and S. K. Ma, Random-Field Instability of the Ordered State of Continuous Symmetry, Phys. Rev. Lett. **35**, 1399 (1975).

[50] M. Levin and T. Senthil, Deconfined quantum criticality and néel order via dimer disorder, Phys. Rev. B **70**, 220403 (2004).

[51] H. Shao, W. Guo, and A. W. Sandvik, Quantum criticality with two length scales, Science **352**, 213 (2016).

[52] I. Kimchi, J. P. Sheckelton, T. M. McQueen, and P. A. Lee, Scaling and data collapse from local moments in frustrated disordered quantum spin systems, Nat. Commun. **9**, 4367 (2018).

[53] Y. Li, G. Chen, W. Tong, L. Pi, J. Liu, Z. Yang, X. Wang, and Q. Zhang, Rare-Earth Triangular Lattice Spin Liquid: A Single-Crystal Study of $YbMgGaO_4$, Phys. Rev. Lett. **115**, 167203 (2015).

[54] Z. Ma, J. Wang, Z. Y. Dong, J. Zhang, S. Li, S. H. Zheng *et al.*, Spin-Glass Ground State in a Triangular-Lattice Compound $YbZnGaO_4$, Phys. Rev. Lett. **120**, 087201 (2018).

[55] S. Dey, E. C. Andrade, and M. Vojta, Destruction of long-range order in noncollinear two-dimensional antiferromagnets by random-bond disorder, Phys. Rev. B **101**, 020411(R) (2020).

[56] R. K. Kaul, R. G. Melko, and A. W. Sandvik, Bridging lattice-scale physics and continuum field theory with quantum Monte Carlo simulations, Annu. Rev. Condens. Matter Phys. **4**, 179 (2013).

[57] A. W. Sandvik, Evidence for Deconfined Quantum Criticality in a Two-Dimensional Heisenberg Model with Four-Spin Interactions, Phys. Rev. Lett. **98**, 227202 (2007).

[58] J. Lou, A. W. Sandvik, and N. Kawashima, Antiferromagnetic to valence-bond-solid transitions in two-dimensional SU(N) Heisenberg models with multispin interactions, Phys. Rev. B **80**, 180414(R) (2009).

[59] T. Senthil, A. Vishwanath, L. Balents, S. Sachdev, and M. P. A. Fisher, Deconfined quantum critical points, Science **303**, 1490 (2004).

[60] T. Senthil, L. Balents, S. Sachdev, A. Vishwanath, and M. P. A. Fisher, Quantum criticality beyond the Landau-Ginzburg-Wilson paradigm, Phys. Rev. B **70**, 144407 (2004).

[61] A. W. Sandvik, Stochastic series expansion method with operator-loop update, Phys. Rev. B **59**, R14157(R) (1999).

[62] A. W. Sandvik, Computational studies of quantum spin systems, AIP Conf. Proc. **1297**, 135 (2010).

[63] J. Guo, G. Sun, B. Zhao, L. Wang, W. Hong, V. A. Sidorov, N. Ma, Q. Wu, S. Li, Z. Y. Meng, A. W. Sandvik, and L. Sun, Quantum Phases of SrCu$_2$(BO$_3$)$_2$ from High-Pressure Thermodynamics, Phys. Rev. Lett. **124**, 206602 (2020).

[64] M. P. A. Fisher, P. B. Weichman, G. Grinstein, and D. S. Fisher, Boson localization and the superfluid-insulator transition, Phys. Rev. B **40**, 546 (1989).

[65] A. V. Chubukov, S. Sachdev, and J. Ye, Theory of two-dimensional quantum Heisenberg antiferromagnets with a nearly critical ground state, Phys. Rev. B **49**, 11919 (1994).

[66] R. B. Griffiths, Nonanalytic Behavior above the Critical Point in a Random Ising Ferromagnet, Phys. Rev. Lett. **23**, 17 (1969).

[67] V. M. Galitski, A. Kaminski, and S. Das Sarma, Griffiths Phase in Diluted Magnetic Semiconductors, Phys. Rev. Lett. **92**, 177203 (2004).

[68] L. Savary and L. Balents, Disorder-Induced Quantum Spin Liquid in Spin Ice Pyrochlores, Phys. Rev. Lett. **118**, 087203 (2017).

[69] L. Chen, D.-W. Qu, H. Li, B.-B. Chen, S.-S. Gong, J. von Delft, A. Weichselbaum, and W. Li, Two temperature scales in the triangular lattice Heisenberg antiferromagnet, Phys. Rev. B **99**, 140404(R) (2019).

[70] K. Riedl, R. Valenti, and S. M. Winter, Critical spin liquid versus valence bond glass in triangular lattice Organic κ-(ET)$_2$Cu$_2$(CN)$_3$, Nat. Commun. **10**, 2561 (2019).

[71] T. Koga, N. Kurita, M. Avdeev, S. Danilkin, T. J. Sato, and H. Tanaka, Magnetic structure of the $S = \frac{1}{2}$ quasi-two-dimensional square-lattice Heisenberg antiferromagnet Sr$_2$CuTeO$_6$, Phys. Rev. B **93**, 054426 (2016).

[72] P. Babkevich, V. M. Katukuri, B. Fåk, S. Rols, T. Fennell, D. Pajić, H. Tanaka, T. Pardini, R. R. P. Singh, A. Mitrushchenkov, O. V. Yazyev, and H. M. Rønnow, Magnetic Excitations and Electronic Interactions in Sr$_2$CuTeO$_6$: A Spin-1/2 Square Lattice Heisenberg Antiferromagnet, Phys. Rev. Lett. **117**, 237203 (2016).

[73] S. Vasala, M. Avdeev, S. Danilkin, O. Chmaissem, and M. Karppinen, Magnetic structure of Sr$_2$CuWO$_6$, J. Phys.: Condens. Matter **26**, 496001 (2014).

[74] H. C. Walker, O. Mustonen, S. Vasala, D. J. Voneshen, M. D. Le, D. T. Adroja, and M. Karppinen, Spin wave excitations in the tetragonal double perovskite Sr$_2$CuWO$_6$, Phys. Rev. B **94**, 064411 (2016).

[75] O. Mustonen, S. Vasala, E. Sadrollahi, K. P. Schmidt, C. Baines, H. C. Walker, I. Terasaki, F. J. Litterst, E. Baggio-Saitovitch, and M. Karppinen, Spin-liquid-like state in a spin-1/2 square-lattice antiferromagnet perovskite induced by d^{10}-d^0 cation mixing, Nat. Commun. **9**, 1085 (2018).

[76] M. Watanabe, N. Kurita, H. Tanaka, W. Ueno, K. Matsui, and T. Goto, Valence-bond-glass state with a singlet gap in the spin-$\frac{1}{2}$ square-lattice random $J_1 - J_2$ Heisenberg antiferromagnet Sr$_2$CuTe$_{1-x}$W$_x$O$_6$, Phys. Rev. B **98**, 054422 (2018).

[77] J. S. Helton, K. Matan, M. P. Shores, E. A. Nytko, B. M. Bartlett, Y. Yoshida, Y. Takano, A. Suslov, Y. Qiu, J.-H. Chung, D. G. Nocera, and Y. S. Lee, Spin Dynamics of the Spin-1/2 Kagome Lattice Antiferromagnet ZnCu$_3$(OH)$_6$Cl$_2$, Phys. Rev. Lett. **98**, 107204 (2007).

[78] A. Iaizzi, K. Damle, and A. W. Sandvik, Field-driven quantum phase transitions in S=1/2 spin chains, Phys. Rev. B **95**, 174436 (2017).

[79] A. Iaizzi, K. Damle, and A. W. Sandvik, Metamagnetism and zero-scale-factor universality in the two-dimensional J-Q model, Phys. Rev. B **98**, 064405 (2018).

[80] J. P. Sheckelton, J. R. Neilson, D. G. Soltan, and T. M. McQueen, Possible valence-bond condensation in the frustrated cluster magnet LiZn$_2$Mo$_3$O$_8$, Nat. Materials **11**, 493 (2012).

[81] K. Kitagawa, T. Takayama, Y. Matsumoto, A. Kato, R. Takano, Y. Kishimoto, S. Bette, R. Dinnebier, G. Jackeli, and H. Takagi, A spin-orbital-entangled quantum liquid on a honeycomb lattice, Nature (London) **554**, 341 (2018).

[82] P. Lampen-Kelley, A. Banerjee, A. A. Aczel, H. B. Cao, M. B. Stone, C. A. Bridges, J.-Q. Yan, S. E. Nagler, and D. Mandrus, Destablization of Magnetic Order in a Dilute Kitaev Spin Liquid Candidate, Phys. Rev. Lett. **119**, 237203 (2017).

[83] S.-H. Do, W.-J. Lee, S. Lee, Y. S. Choi, K.-J. Lee, D. I. Gorbunov, J. Wosnitza, B. J. Suh, and K.-Y. Choi, Sort-range quasistatic order and critical spin correlations in α-Ru$_{1-x}$Ir$_x$Cl$_3$, Phys. Rev. B **98**, 014407 (2018).

[84] S.-H. Do, C. H. Lee, T. Kihara, Y. S. Choi, S. Yoon, K. Kim, H. Cheong, W.-T. Chen, F. Chou, H. Nojiri, and K.-Y. Choi, Randomly Hopping Majorana Fermions in the Diluted Kitaev System α-Ru$_{0.8}$Ir$_{0.2}$Cl$_3$, Phys. Rev. Lett. **124**, 047204 (2020).

[85] S.-H. Baek, H. W. Yeo, S.-H. Do, K.-Y. Choi, L. Janssen, M. Vojta, and B. Büchner, Observation of a gapless spin liquid in a diluted Kitaev honeycomb material, arXiv:2005.13836.

[86] W. Hong, L. Liu, C. Liu, X. Ma, A. Koda, X. Li, J. Song, W. Yang, J. Yang, P. Cheng, H. Zhang, W. Bao, X. Ma, D. Chen, K. Sun, W. Guo, H. Luo, A. W. Sandvik, and S. Li, Extreme suppression of antiferromagnetic order and critical scaling in a two-dimensional random quantum magnet, arXiv:2006.15749.